Supporting Online Material for

GABAergic Hub Neurons Orchestrate Synchrony in Developing Hippocampal Networks

P. Bonifazi, M. Goldin, M. A. Picardo, I. Jorquera, A. Cattani, G. Bianconi, A. Represa, Y. Ben-Ari, R. Cossart*

*To whom correspondence should be addressed. E-mail: cossart@inmed.univ-mrs.fr

Published 4 December 2009, *Science* **326**, 1419 (2009)
DOI: 10.1126/science.1175509

This PDF file includes:

Materials and Methods
Figs. S1 to S5
References

Other Supporting Online Material for this manuscript includes the following: (available at www.sciencemag.org/cgi/content/full/326/5958/1419/DC1)

Movie S1

Supporting Online Material

METHODS

Slice preparation and calcium imaging

Transverse slices of hippocampus (350 μm thick) were prepared from 5 to 7-day-old (P5-7) Wistar rats (n = 86 slices) and GAD67-KI mice (n= 66 slices) using a vibratome in ice-cold oxygenated modified artificial cerebrospinal fluid (0.5 mM $CaCl_2$ and 7 mM $MgSO_4$; NaCl replaced by an equimolar concentration of choline). Slices were then transferred for rest (around 1 hr) in oxygenated normal ACSF containing (in mM): 126 NaCl, 3.5 KCl, 1.2 NaH_2PO_4, 26 $NaHCO_3$, 1.3 $MgCl_2$, 2.0 $CaCl_2$, and 10 D-glucose, pH 7.4. For AM-loading, slices were incubated in a small vial containing 2.5 ml of oxygenated ACSF with 25 μl of a 1 mM Fura2-AM solution (in 100% DMSO) for 20–30 min. Slices were incubated in the dark, and the incubation solution was maintained at 35°–37°C. Slices were perfused at a rate of 3 ml/min with continuously aerated (O_2/CO_2-95/5%) normal ACSF at 35-37°C. Imaging was performed with a multibeam multiphoton pulsed laser scanning system coupled to a microscope as previously described (*1*). Images were acquired through a CCD camera, which typically resulted in a time resolution of 50 to 150 ms per frame (4X4 binning, pixel size: 1.2 μm). Typical movie size was 3000 to 4000 frames i.e. 150 to 600 seconds. Slices were imaged using a low-magnification, high numerical aperture objective (20X, NA-0.95) or a lower-magnification objective (10X, NA-0.3). The size of the imaged field was typically: 430 x 380 μm^2 at 20X magnification and four times that area at 10X magnification. Imaging depth was on average 80 μm below the surface (range: 50-100 μm). Given the average GDP frequency (0.03-0.5 Hz) continuous recordings of ten minutes were necessary to sample at least 15 GDPs.

Electrophysiology

For this study, a total of 142 neurons were recorded while imaging. Only 45 experiments (n= 33 rats and 13 mice) were considered. The other experiments (n = 97) were discarded because they did not comply either one of the following criteria: (1) stable electrophysiological recordings at resting membrane potential (Vrest, n = 15) i.e. the holding current did not change by more than 15 pA; (2) stable spontaneous network dynamics measured with calcium imaging, i.e. the coefficient of variation of the inter-GDP interval did not exceed 1 (n = 17); (3) complete biocytin labelling of the recorded cell (n = 22); (4) good quality calcium imaging while recording, i.e. no movement of the slice and a change in baseline fluorescence not exceeding 10% (n = 6); (5) detectable calcium transients in the recorded neuron after patching (n = 37). Neurons were recorded using the patch-clamp technique in the whole-cell configuration. The composition of the intracellular solution for current-clamp recordings was: 130 mM K-methylSO_4, 5 mM KCl, 5 mM NaCl, 10 mM HEPES, 2.5 mM Mg-ATP and 0.3 mM GTP. No correction for liquid junction potential was applied. The osmolarity was 265–275 mOsm, pH 7.3. Microelectrodes resistance was 4-8 MOhms. Uncompensated access resistance was monitored throughout the recordings. Values below 20MOhms were considered acceptable and the results were discarded if it changed by more than 20%. Whole cell measurements were filtered at 3 kHz using a patch-clamp amplifier. Recordings were digitized online (10 kHz) with an interface card to a personal computer and acquired using Axoscope 7.0 software. For paired recordings, 'follower neurons' were recorded in voltage-clamp mode using an intracellular solution composed as follows: 120 mM Cs-gluconate, 10 mM MgCl2, 0.1mM CaCl2, 1mM EGTA, 5mM Na2 adenosine triphosphate, 10 mM HEPES. With this solution Glutamate-R-mediated postsynaptic currents (PSCs) reversed at +10mV while GABAA-R-mediated PSCs reversed at -60 mV. Neurons were successively held at both +10 and -70 mV. Liquid junction potential value was -16.8 mV but no correction was applied. Presynaptic neurons were recorded in current-clamp and synaptic connections were tested by

applying repetitive current injections inducing trains of 3 spikes at 10 Hz every 10 seconds. In order to reveal potentially triggered PSCs, voltage clamp recordings were averaged across stimulation trials including failures. If IPSCs were triggered by stimulation at +10 mV, we next applied antagonists for AMPA/KA and NMDA-Rs (NBQX 10 μM and D-APV 40μM) in order to confirm the involvement of GABAA-Rs in their generation. EPSPs were detected and analyzed using the MiniAnalysis software. Synchronization between optical and electrical signals was achieved by feeding simultaneously the interface card with the trigger signals for each movie frame and the electrophysiological recordings. For most stimulation experiments, the movie acquisition time was separated evenly between (1) a resting period (~ 3 minutes) during which the cell was held close to resting membrane potential (i.e. zero current injection); (2) a stimulation period (~3 minutes) during which phasic or tonic stimulation protocols were applied (see below); (3) a recovery period (~3 minutes) where the cell was brought back to resting membrane potential. Two separate stimulation protocols were used: (1) a phasic stimulation: suprathreshold current pulses (amplitude: 75-100 pA, duration: 200 ms) repeated at 0.1-0.2 Hz i.e. the typical frequency range of spontaneous GDPs; (2) tonic stimulation: continuous positive (~+20 pA) or negative (~-20 pA) current injections bringing the cell to a membrane potential where it fired continuously or was completely silenced, respectively.

Vrest was measured as the membrane potential baseline value obtained in current-clamp mode in the absence of current injection. The action potential threshold (Vthreshold) and amplitude were measured offline using Clampfit. Note that the action potential amplitude can be small in some of the recorded cells (see for example Fig. 3C2). This is a common property of immature neurons as there is a very large increase in the amplitude of inward sodium currents between late embryonic and early postnatal stages of cortical development (*2*). In

addition, because the input resistance of developing neurons is large, it was necessary to correct both Vrest and Vthreshold using the following formula (*3, 4*):

V =Vmes*Rseal/ (Rseal – Rin) where Vmes is the measured potential; Rseal is the seal resistance; and Rin is the input resistance.

Morphology

Slices were processed for the detection of biocytin-filled neurons according to a previously established procedure (*5*). Briefly, slices were fixed overnight at 4 °C in a solution containing 4% paraformaldehyde in 0.1 M phosphate buffer (PB, pH 7.4). To neutralize endogenous peroxidase, slices were pretreated for 30 minutes in 1% H_2O_2. After several rinses in saline phosphate buffer (0.01 M PBS, pH 7.4), slices were incubated for 24 hours at room temperature, in 1/100 avidin-biotin peroxidase complex diluted in PBS containing 0.3% Triton X-100. After 30 minutes rinses in PBS, slices were processed with 0.04% 3-3'-diaminobenzidine-HCl and 0.006% H_2O_2 diluted in PBS. The visualization of neurons recorded in GADGFP-KI mouse slices was obtained using CY3-conjugated streptavidin (1:500). Post-hoc analysis was performed using a confocal microscope. Stacks of optical sections were collected for computer-assisted neuron reconstructions.

Twenty labelled neurons were reconstructed for morphometric analysis with a computer-assisted system attached to a microscope. Morphological variables thus obtained included: total dendritic and axonal lengths, total dendritic and axonal surfaces, total dendritic and axonal volumes and total number of dendritic and axonal terminals. The total surface of dendrites or axons (branched structures) is an estimated value calculated by the software. They are computed by modelling each piece of each branch as a frustum i.e. the shape formed by a right circular cone that has been truncated. The total length of dendrites or axons is the sum of the lengths of all the branches.

Cluster analysis for morphological data was performed using Statistica software. The term "cluster analysis" refers to a set of multivariate exploratory statistical methods that group objects (cases) of a data set based on their degree of similarity. All cases are first plotted in a multidimensional space defined by all the measured variables.

A certain measure of proximity is chosen (distance), and clusters are eventually formed by the cases that fulfil the criteria of the clustering method selected. Our analysis was performed with Euclidean distances by using Ward's method. According to Ward's method, cases are assigned to clusters so that the variance (sum of squared deviations from the mean) within each cluster is minimized. This method resulted in well-defined groups in this study.

Data Analysis

Group measures are expressed as means ± SEM; error bars also indicate SEM unless stated otherwise. The statistical significance was assessed with the Student's t-test or Mann-Whitney in the case where the normality distribution test failed (Kolmogorov-Smirnov test with Lilliefors' correction, $p < 0.05$). The level of significance was set at $P < 0.05$. Experiments performed in mice and rats were first analyzed separately. No significant statistical difference for the power law scaling factor was observed (Student's t-test, $p<0.05$), therefore data were pooled together.

Signal detection and network topology: Analysis of the calcium activity was first performed online in about 20 minutes considering a 4000 frames movie. We used custom designed software (*1, 6*) which allowed: 1) automatic identification of loaded cells; 2) measuring the average fluorescence transients from each cell as a function of time 3) detecting the onsets and offsets of calcium signals 4) reconstructing the functional connectivity of the imaged network. The latter operation was based on pair-wise correlation analysis. When the firing onset of cell A preceded in a repetitive way the activation of cell B, we established a link, i.e. a functional connection, directed from A to B. In order to reveal these temporal correlations,

the firing onsets of each neuron were converted into a binary (0 - 1) time series of length N, where N is the number of frames in the movie and ones represent the onset times. Given the onset times of neuron A, we calculated the distribution of events of neuron B occurring at different time lags (between -800 ms and +800 ms). This measure is equivalent to the poststimulus time histogram of cell B but centered on the firing onsets of cell A (*7*). We used both the Student's t-test and the Kolmogorov-Smirnov test ($p<0.01$) to exclude that the events distribution was significantly different from a Gaussian centred at zero and from a uniform distribution, respectively. In this way, we excluded cases where the activation of two neurons was completely uncorrelated (uniform distribution) or synchronous (Gaussian centred at zero). Zero delay correlations were discarded first because they cannot be resolved using our temporal resolution. Second, because most of the activity in the cells occurs during GDPs and including these connections would result in a fully connected network. Given the early stage of maturation, this is not biologically feasible and realistic for the networks we studied. When these two conditions were fulfilled, a link was directed either from A to B, if the average time lag was greater than zero, or from B to A if it was lower than zero. By applying this procedure to all possible pairs of neurons, we were able to reconstruct online the functional topology of the imaged network within 20 minutes after the acquisition of the calcium movie. In this way, it was possible to target for electrophysiological recordings neurons with a known number of incoming and outgoing connections. For all the experiments included here (45 slices), offline manual analysis was performed in addition, to correct online errors in cell or signal detection. For all targeted neurons ($n = 45$), the error in the total number of outgoing connections due to the online analysis was $15 \pm 5\%$.

In order to colour-code functional connectivity maps, we built a binary matrix from the calcium image for which a value of one was assigned to the pixels included in the contours of

functionally connected cells. For an easier visualization, a convolution with a Gaussian of unitary amplitude and 8 μm radius was performed.

In order to compare the connectivity distributions of outgoing links between different networks, we considered the fraction of active cells that each neuron was connected with. Only cells having at least one link (output or input) were considered in the analysis. Power laws ($\sim x^{-\gamma}$) were estimated for each network using a fit on the cumulative distribution of the fraction of output links (*8*). The goodness of the fit was tested using standard Kolmogorov-Smirnov test according to (*9*). For the networks imaged using a 20X objective, power laws were observed in 41 out of 45 cases. In the figures, the distribution of the data pooled over all slices is shown.

Analysis of network synchronizations. Network synchronizations (GDPs) were detected as synchronous onsets peaks including more neurons than expected by chance, as previously described (*6*). In order to compare the dynamics of GDPs occurring within the same network, analysis was focused on a one second time window centred on the coactivation peak (time zero). An average GDP profile was thus calculated. The time window between 10 and 100% of the average peak size was used as an estimate of the build up duration. To reveal if a characteristic pattern of cells was recruited in the GDP build-up period, we identified cells activated within 350 ms before the peak of synchrony. Similarity between cell patterns was measured using K-Means clustering. We assigned a binary format to the data (1: cells activated/ 0: cells not activated) and we used the hamming distance to identify clusters. A characteristic pattern was identified for a cluster with an average cosine distance greater than 0.2. Unlike hamming distances which assign equivalent weight to activated and not-activated cells, the cosine distance measures only the similarity between patterns of activated cells (to which we assigned value 1).

"Time-correlation" graph. In order to estimate the average temporal correlation and the relative time of activation of each cell within these characteristic GDPs, we included only event onsets occurring within a 1 second time window, centred on the synchronization peaks. Other events were excluded. Similar to the above, we calculated the distribution of events in the network occurring at different time lags respective to the firing onsets of a given neuron. In this way, for every neuron, we estimated the average firing time-lag compared to other cells and the average correlation (peak value divided by the area of the distribution).

Cell-network interaction. To establish whether the stimulation of a single neuron was able to influence the occurrence of GDPs we used the three different metrics described below. Resting conditions were measured when holding the cell at resting membrane potential (zero current) while performing calcium imaging.

(1) The average inter GDP intervals (<iGDPi>) in resting conditions and during stimulation were compared. The distributions of <iGDPi> were best fitted by Normal or Poissonian distributions depending on the network (Kolmogorov-Smirnov test, $p > 0.05$). Significant cell-network interaction occurred when the <iGDPi> distributions during resting conditions and during stimulation were statistically different as assessed using either the Student's t-test or the Mann-Whitney test for Normal and Poissonian distributions respectively. $P<0.05$ was considered significant.

(2) In order to evaluate whether a phasic stimulation with period *t* was able to trigger GDPs within 1 sec following the stimulation, we first excluded cases in which the number of GDPs occurring within this time window did not exceed the value expected by chance for a uniform distribution ($p<0.05$), i.e. $(n*f+2*\sqrt{(n*f)})$, where f is the average frequency of GDPs and n is the number of stimulation trials. Because the period *t* was typically comparable to the <iGDPi>, in order to avoid artefacts due to the intrinsic periodicity of GDPs, the distribution of GDPs between two consecutive stimuli was compared to that obtained for virtual null

amplitude stimuli of identical periodicity *t* applied during resting conditions. Significant cell-network interaction occurred when the two distributions were statistically different (Kolmogorov-Smirnov, $p < 0.05$ was considered significant).

(3) <iGDPi> during resting conditions was used as a reference period of a harmonic oscillator mimicking the rhythm of GDPs. The phase of the expected GDPs (eGDPs), i.e. generated by the harmonic oscillator, was compared to that of the real GDPs (rGDPs) occurring during the entire recording. The phase of each rGDP was set to zero at the peak of synchronous activation and increased linearly reaching 2π at the peak of the next rGDP. By subtracting the phase of rGDPs from eGDP, we could instantaneously measure the effect of phasic stimulation. Only if the difference between expected and observed cycles did not exceed ±2 cycles during resting conditions, was this procedure used to evaluate cell-network interaction. A cell was considered as significantly influencing network dynamics according to that metric if the maximal fluctuation between the phase differences during stimulation exceeded three times the standard deviation of the fluctuations in resting conditions ($p < 0.01$).

Effective connectivity map. In order to identify cells in the network responding to phasic stimulations, for each cell we first calculated the average fluorescence change across trials in a time window between -1 and 1 seconds centred on the time of the stimulus. Cross-correlation between the average calcium signal of the cell and the calcium signal of the stimulated cell was calculated at time lags varying between -1 and +1 s. If the maximum of the cross-correlation exceeded 0.5 and occurred at positive times, indicating that the activation of the cell followed the stimulation, the cell was considered as responding to the stimulation. In order to colour-code the effective connectivity map, we built a matrix from the calcium image of the slice and we assigned to each cell its maximal cross-correlation value. The image was then convolved with a Gaussian of unitary amplitude and 8 μm radius.

References and Notes

1. V. Crepel *et al.*, *Neuron* **54**, 105-120 (2007).
2. W. J. Moody, M. M. Bosma, *Physiol Rev.* **85**, 883-941 (2005).
3. S. Rheims *et al.*, *J. Neurophysiol.* **100**, 609-619 (2008).
4. R. Tyzio *et al.*, *J. Neurophysiol.* **90**, 2964-2972 (2003).
5. R. Cossart *et al.*, *Hippocampus* **16**, 408-420 (2006).
6. C. Allene *et al.*, *J. Neurosci.* **28**, 12851-12863 (2008).
7. G. Palm, A. M. Aertsen, G. L. Gerstein, *Biol. Cybern.* **59**, 1-11 (1988).
8. M. E. J. Newman, *arXiv:cond-mat/0412004v3* (2006).
9. M. C. Gonzalez, C. A. Hidalgo, A. L. Barabasi, *Nature* **453**, 779-782 (2008).

Supplemementary Figure Legends

Fig. S1.

A. Rasterplot of the onsets of calcium events in a movie acquired at low magnification (10X, frame rate: 6.67 Hz). The spontaneous activity of about 1000 neurons across the entire CA3 area could be simultaneously recorded. Note the occurrence of several spontaneous GDPs appearing as broken vertical lines in the raster plot. Imaged region and detected contours of the imaged area are represented in Fig. 1A1&2. **B. 1.** Simultaneous calcium events recorded in 45 cells (gray traces) compared to the calcium transient measured in a HC neuron (red trace). Frame rate: 13.34 Hz. The onset of the HC neuron precedes the large majority of activity onsets in other recorded neurons. **2.** Distribution of activation times for nine neurons relative to the activation times of the HC neuron (red trace in 1). These distributions peak at positive values in all neurons but one, i.e. the HC cell is consistently active before the others. X axis: time in milliseconds; Y axis: number of occurrences. **C.** Simultaneous cell-attached and calcium recordings showing the strong correlation between action potential firing and fluorescence changes (frame rate: 10 Hz) in a HC neuron. Action potential firing in the HC neuron occurs prior to GDPs (*). Upward current fluctuations correspond to single-channel activity.

Fig. S2. Stimulation of CA3 pyramidal cells does not significantly affect network dynamics independently from their connectivity index.

A&B. 1. Green arrows in the pooled power law indicate the percentage of output links (see Fig. 1B) for the recorded LC (A1) and HC (B1) pyramidal neurons. Contour plots show the position (green filled contour) and output connections (gray lines) of the neurons. sl: stratum lucidum; so: stratum oriens. Scale bar: 100µm. **2.** Phasic current-clamp stimulation (200ms pulses of 75 pA current every 10 seconds, gray area) of the LC (A2) or HC (B2) pyramidal

neuron did not affect the occurrence of GDPs detected by imaging the calcium activity ($p>0.1$). The interval between GDPs is plotted as a function of time and does not change during stimulation. Values are expressed relative to the average GDP frequency outside the stimulation period. **3.** Neurolucida reconstructions of the recorded cells on a schematic representation of the hippocampus reveals a pyramid-like morphology (dendrites in black) displaying a local (A3) or extended (B3) axonal arborisation (green). Dotted rectangle indicates imaged region. Scale bar: 500 μm.

Fig. S3. Hub neurons are GABAergic cells with widespread axonal arborisations located at the pyramidal cell layer borders.

A. Superimposed Neurolucida reconstructions of six hub (1) and six (2) LC interneurons on a schematic representation of the hippocampus. Scale bar: 500μm. Axonal arborisations are indicated in colour and dendrites in black. **B. 1.** Photomicrograph of a biocytin-filled hub interneuron in the CA3c hippocampal region from a GADGFP-KI mouse. Imaged area is outlined. Scale bar: 100μm. **2.** Left image shows the localization of EGFP+ neurons in the imaged region. Recorded hub neuron was EGFP+ (arrow). Right: colour coded representation of the functional connectivity map of the hub neuron (red: high connection density) overlaid with the contour plot of imaged cells and with the axonal morphology (red) of the hub cell in that region. EGFP+ cells are outlined in green and the soma of the hub neuron is marked by an asterisk; a.u.: arbitrary units. **3.** Radial distribution of HC neurons relative to the stratum oriens/pyramidal cell layer (distance zero, 45 slices) is bimodal and displays two peaks corresponding to the two opposite borders of the pyramidal cell layer. **4.** Histogram representing the distribution of EGFP+ cells as a function of connectivity index (HC region is filled).

Fig. S4. Parallel between "functional" and "effective" connectivity in HC Neurons

Comparison of "functional connectivity" (i.e. based on temporal correlations of spontaneous calcium events, left) and "effective connectivity" (i.e. cells responding to single-cell phasic stimulation, right, see S.O.M.) for a HC interneuron (**A**) and a HC pyramidal cell (**B**). Left contour plots show the position (red filled contour) and functional output connections (gray lines) of the recorded neuron. Scale bar: 100 μm. Right colour coded maps represent the correlation between the calcium transient evoked in the stimulated cell and in each single imaged cell. For comparison purposes, the functional output connections (yellow lines) are superimposed to the effective connectivity map. Maps overlapped by 53% in the HC interneuron and only 10% for the HC pyramidal cell.

Fig. S5. Hub neurons can be monosynaptically connected to follower neurons

A. Contour plot shows the position (red filled contour) and output connections (gray lines) of the illustrated HC neuron. Green filled contour indicates the position of a functionally connected neuron (FC) targeted for electrophysiological recordings. sl: stratum lucidum; so: stratum oriens. Scale bar: 100 μm. Left histogram plots the distribution of activation times for the FC neuron relative to the activation times of the hub neuron. This distribution peaks at positive values indicating that the HC cell is consistently active before the FC neuron. Frame rate: 6.67 Hz. **B.** Peristimulus time histogram showing the average fraction of active cells following single-HC cell stimulation. A significant peak of synchrony (marked by *) was detected following stimulation ($p<0.05$, see S.O.M.). **C.** Confocal image of the immunolabelled HC (red *) and FC (green *) neuron. Arrows indicate the dense axonal innervation originating from the HC neuron. Right: Partial Neurolucida reconstruction of the axonal arborisation of the HC neuron (red). Arrows indicate two putative synaptic contacts with the soma of the FC neuron (green). Scale bar: 20 μm. D. Paired recordings from the HC (red traces) and the FC neuron (green). HC neuron was recorded in current-clamp mode at

Vrest (-60 mV) while the FC neuron was voltage-clamped at the reversal potential for glutamatergic currents (+10 mV). **1.** Spontaneous activity of both cells during a GDP (open square). Action potential firing in the HC neuron precedes synchronization. Most action potentials in the HC neuron are time-locked with sIPSCs in the FC cell. **2.** In the presence of AMPA/KA- and NMDA-R antagonists (NBQX 10μM and D-APV 40μM), evoked action potential firing in the HC neuron triggers IPSCs (*) in the FC neuron that can be visible on single trials (top) as well as when averaging across trials including failures (bottom trace, n = 50 trials). This confirms that cells are directly synaptically coupled.

Movie S1. Movie of the spontaneous multineuron calcium activity in a CA3 rat slice simultaneously recorded with membrane potential changes in a hub neuron (current-clamp mode, red trace; same neuron as in Fig. 3C). Cells were loaded with Fura2-AM and the slice was imaged using multibeam two-photon excitation with a 20X objective. Bottom blue histogram shows the fraction of active cells as a function of time (in movie frames; Acquisition rate was 150 msec/frame). Peaks in the fraction of coactive cells correspond to GDPs. Note that synchronization is completely prevented by sustained membrane potential depolarization of the hub cell whereas the global level of single-cell activity is maintained during stimulation. Significant effect on network synchronization started at movie frame # 1600 ($p<0.05$, see S.O.M.). Network synchrony resumes when bringing the hub cell back to resting conditions.

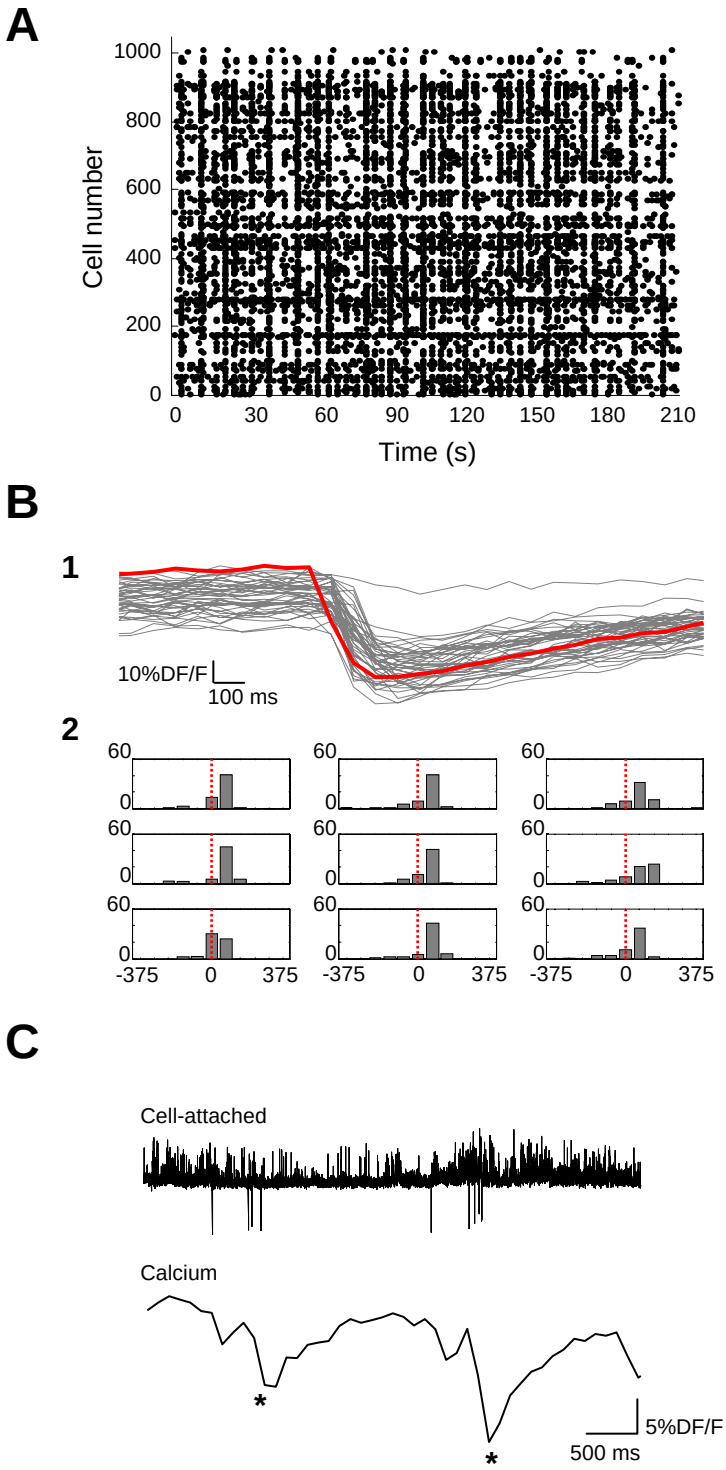
A
1000
800
600
400
200
0
Cell number
0
30
60
90
120
150
180
210
Time (s)
B
1
10%DF/F
100 ms
2
60
0
-375
0
375
C
Cell-attached
Calcium
*
*
5%DF/F
500 ms

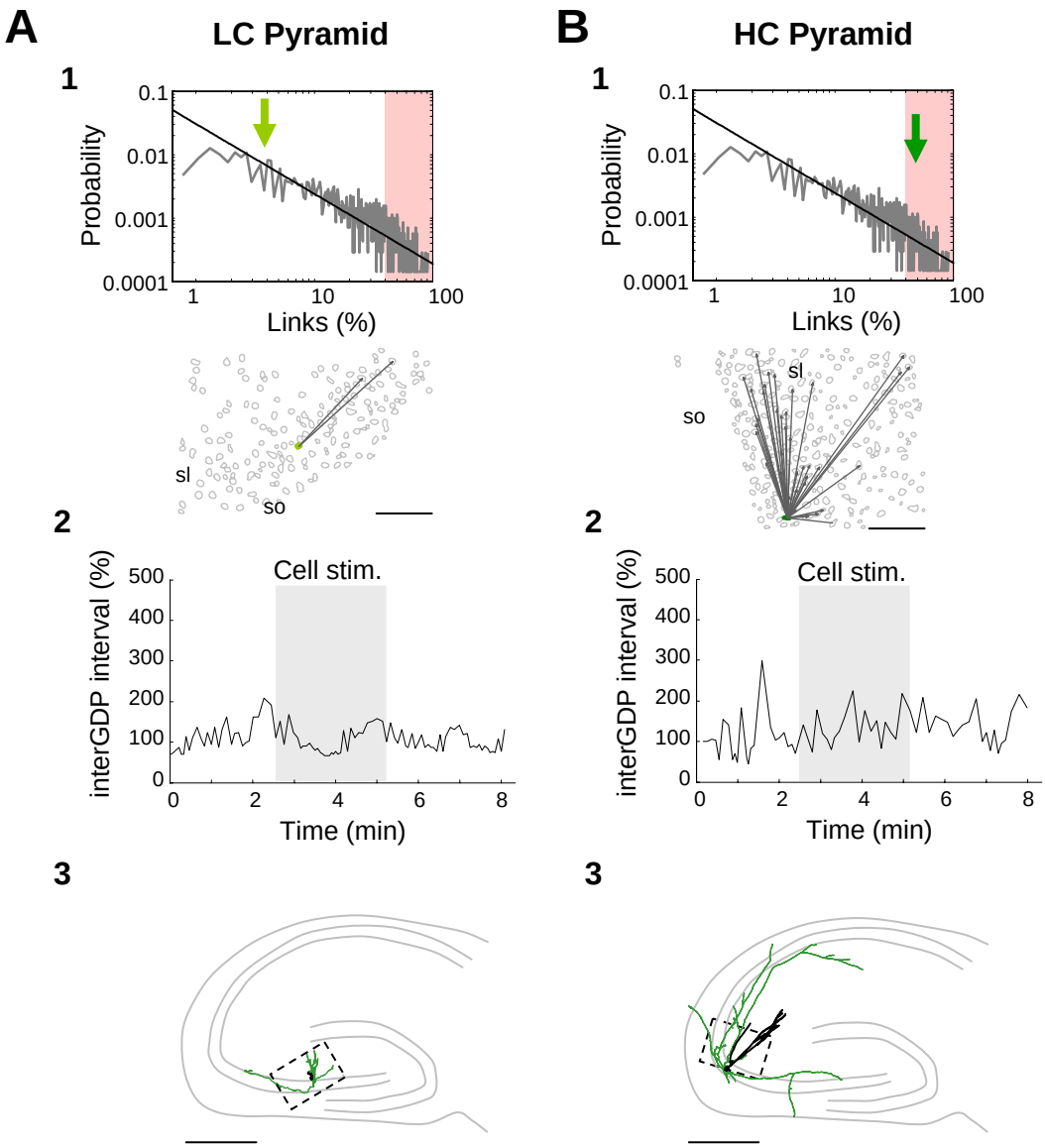
A
LC Pyramid
1
Probability
0.1
0.01
0.001
0.0001
1
10
100
Links (%)
sl
so
2
interGDP interval (%)
500
400
300
200
100
0
Cell stim.
0
2
4
6
8
Time (min)
3
B
HC Pyramid
1
Probability
0.1
0.01
0.001
0.0001
1
10
100
Links (%)
sl
so
2
interGDP interval (%)
500
400
300
200
100
0
Cell stim.
0
2
4
6
8
Time (min)
3

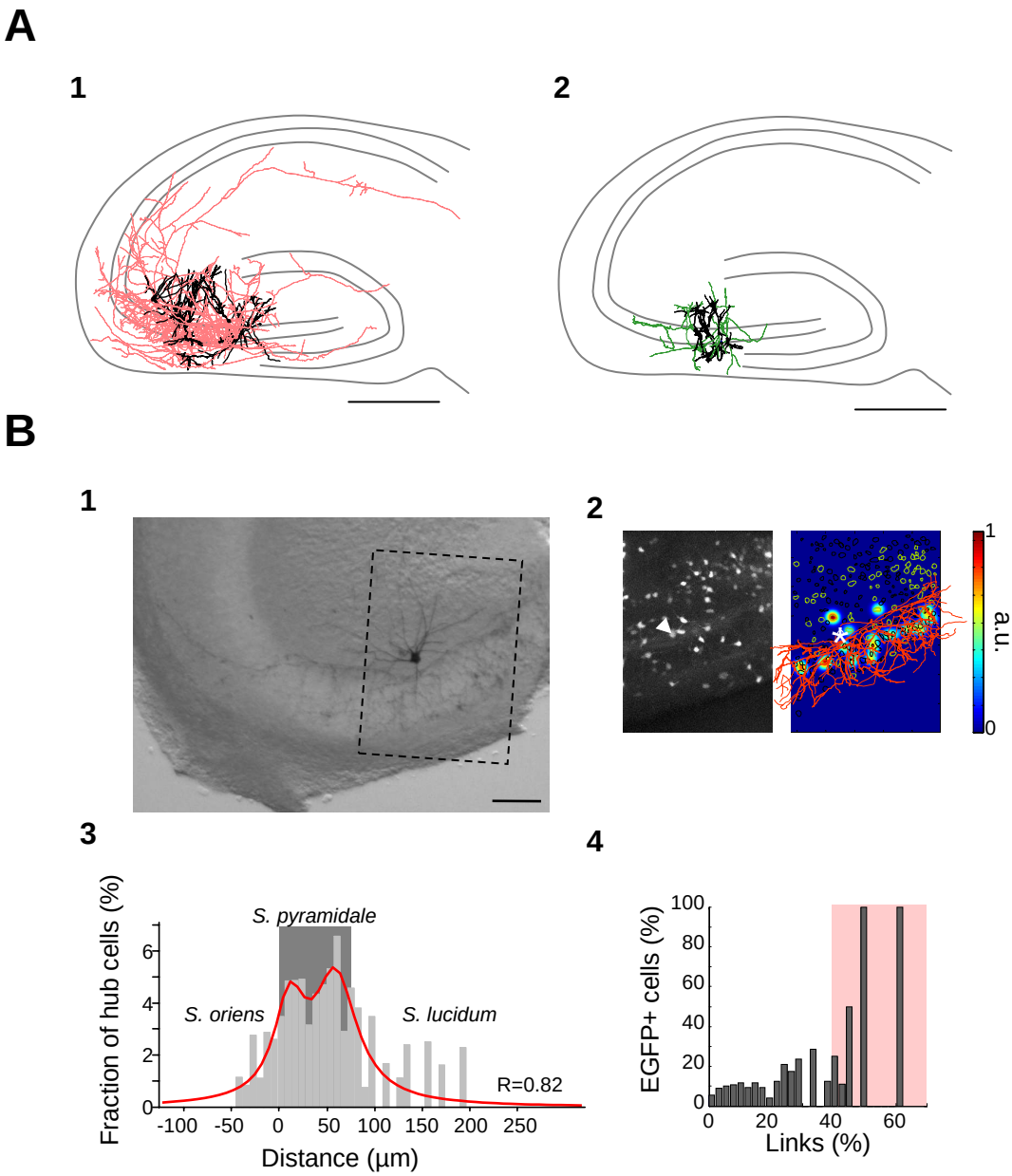
A
1
2
B
1
2
1
a.u.
0
3
S. pyramidale
S. oriens
S. lucidum
R=0.82
Fraction of hub cells (%)
Distance (µm)
4
EGFP+ cells (%)
Links (%)

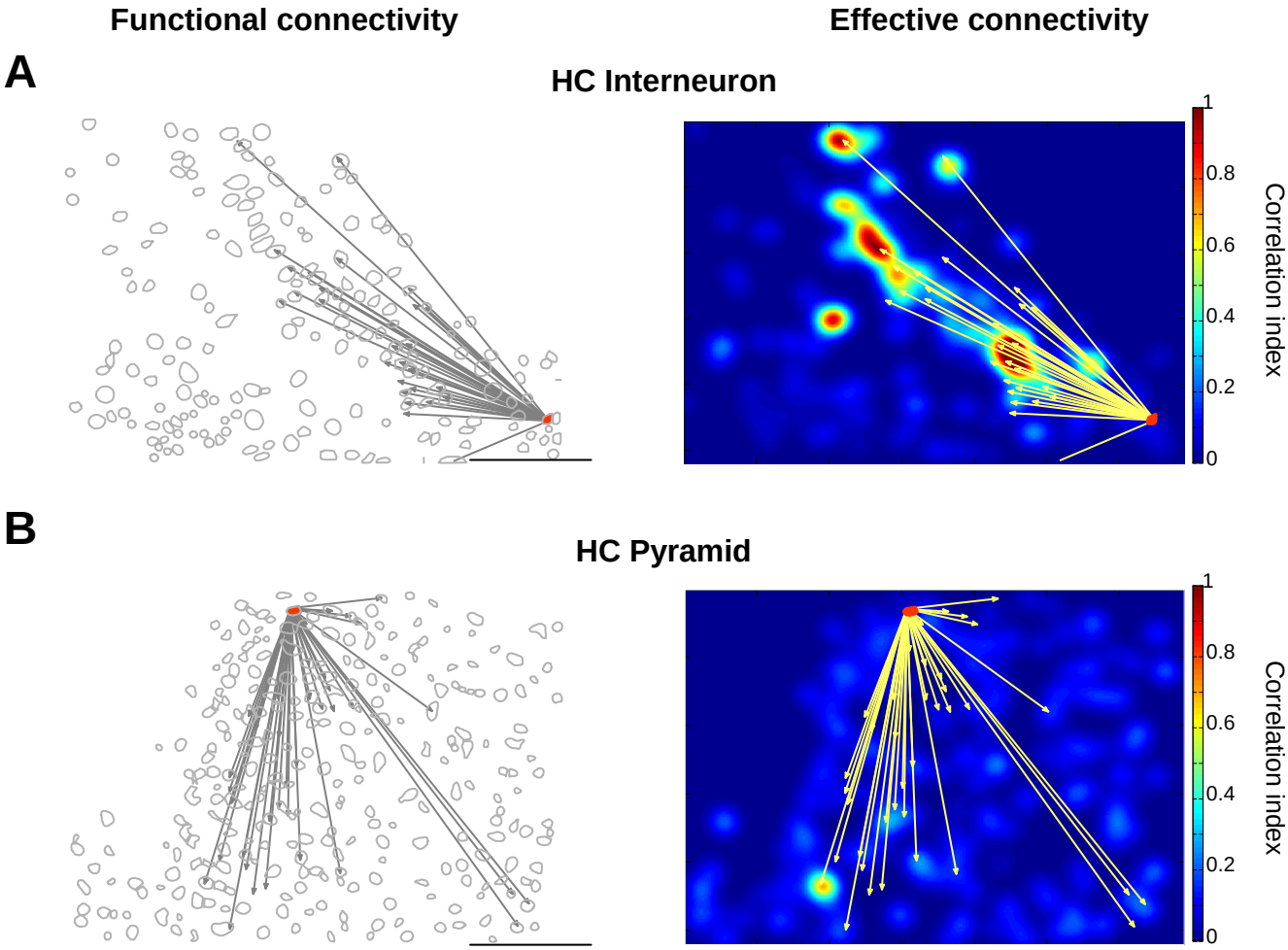
Functional connectivity
Effective connectivity
A
HC Interneuron
B
HC Pyramid
1
0.8
0.6
0.4
0.2
0
Correlation index

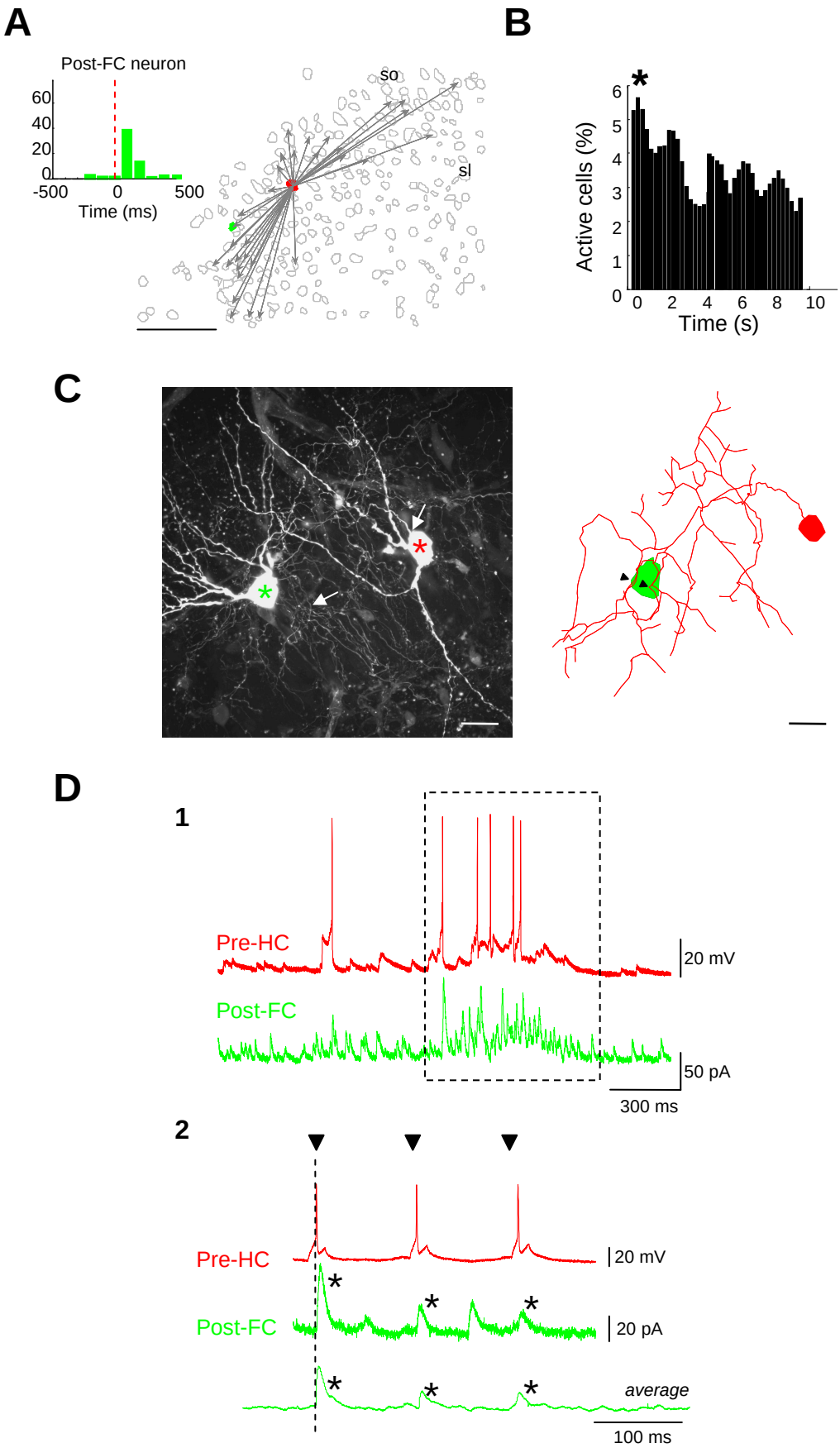
A
Post-FC neuron
60
40
20
0
-500
0
500
Time (ms)
so
sl
B
Active cells (%)
6
5
4
3
2
1
0
0
2
4
6
8
10
Time (s)
C
D
1
Pre-HC
20 mV
Post-FC
50 pA
300 ms
2
Pre-HC
20 mV
Post-FC
20 pA
average
100 ms